Original Article

Right ventricular function and determining factors of dysfunction in ST-segment-elevation myocardial infarction: a cross-sectional study with cardiac magnetic resonance imaging (MRI)

Yanan Zhao[1], Jianing Cui[1], Xinghua Zhang[1], Jinfeng Li[1], Junjie Yang[2], Tao Li[1]

[1]Department of Radiology, The First Medical Center of Chinese People's Liberation Army General Hospital, Beijing, China; [2]Senior Department of Cardiology, The Sixth Medical Center of Chinese People's Liberation Army General Hospital, Beijing, China

Contributions: (I) Conception and design: Y Zhao, J Cui, T Li; (II) Administrative support: T Li; (III) Provision of study materials or patients: Y Zhao, J Cui, J Li; (IV) Collection and assembly of data: Y Zhao, J Cui, X Zhang, T Li; (V) Data analysis and interpretation: Y Zhao, J Cui, X Zhang, J Yang, T Li; (VI) Manuscript writing: All authors; (VII) Final approval of manuscript: All authors.

Correspondence to: Tao Li, MD. Department of Radiology, The First Medical Center of Chinese People's Liberation Army General Hospital, No. 28, Fuxing Road, Haidian District, Beijing 100853, China. Email: litaofeivip@163.com.

Background: Over the past few decades, left ventricular (LV) dysfunction in ST-segment elevation myocardial infarction (STEMI) patients has been the focus of research. Recently, co-occurring right ventricular (RV) dysfunction has received more attention in clinical practice. We aimed to assess RV function using cardiac magnetic resonance (CMR) imaging and identify factors that may contribute to RV dysfunction in STEMI patients.

Methods: We retrospectively studied 189 patients with STEMI who underwent CMR 1–7 days after successful percutaneous coronary intervention (PCI). The ejection fraction (EF), wall thickening rate (WTR), peak radial strain (RS), circumferential strain (CS) and longitudinal strain (LS) of the LV, interventricular septum (IVS) and RV were measured with cine images. The location and extent of the infarct were determined using late gadolinium enhancement (LGE) imaging. The differences of function between STEMI patients with right ventricular ejection fraction (RVEF) <50% and those with RVEF ≥50% were compared using an independent-sample *t*-test. Linear regression analyses were used to determine independent predictors of RVEF.

Results: RVEF <50% was observed in 32.28%% STEMI patients, who also demonstrated significantly lower left ventricular ejection fraction (LVEF), WTR, RS, CS, LS and larger infarct sizes than those with RVEF ≥50%. Patients with RVEF <50% also demonstrated a higher incidence of RV infarction, higher RV end-systolic volume (ESV) index, and lower RV RS and CS. Multivariable linear regression analysis revealed LV EF, IVS WTR and IVS RS as significant predictors for RVEF, while male gender, the culprit lesion in the right coronary artery (RCA), peak troponin were negative predictors for RVEF. Notably, peak troponin, LV EF, LV RS, LV CS, LV WTR, and IVS WTR demonstrated higher area under the curve (AUC) values for predicting RV dysfunction.

Conclusions: RV dysfunction was detected in 32.28% of STEMI patients. Patients with acute STEMI and RVEF <50% had impaired LV and IVS functions. Systolic function of the LV and IVS, peak troponin, and culprit lesions in the RCA were independent predictors of RV dysfunction in STEMI patients.

Keywords: Cardiac magnetic resonance (CMR); right ventricular dysfunction (RV dysfunction); ST-segment-elevation myocardial infarction (STEMI)

Submitted Dec 20, 2023. Accepted for publication May 11, 2024. Published online Jun 11, 2024.
doi: 10.21037/qims-23-1804
View this article at: https://dx.doi.org/10.21037/qims-23-1804

Introduction

Patients with acute ST-segment-elevation myocardial infarction (STEMI) and impaired left ventricular (LV) function have been the focus of considerable research and risk assessments over the past few decades (1,2). However, in clinical practice, it has been observed that some STEMI patients not only exhibit impaired LV function, but also suffer from right ventricular (RV) dysfunction. A reduced RV ejection fraction (EF) in patients with STEMI can lead to inadequate preloading of the LV and a corresponding decrease in cardiac output, resulting in systemic hypoperfusion. Therefore, when RV dysfunction occurs in patients with STEMI, timely assessment and appropriate treatment adjustments are crucial to prevent further complications. In addition to conventional revascularization and anticoagulant therapy, these patients should receive sufficient amounts of intravenous fluids, avoid medications that reduce the preload (such as opioids, nitrates, and diuretics), and abstain from taking medications with negative inotropic and chronotropic effects (3,4). It is also important to explore which factors contribute to RV dysfunction in STEMI. This would have significant implications to actively prevent the occurrence of right heart dysfunction.

Echocardiography has been used to evaluate the cardiac function in previous clinical and research settings. However, echocardiography has limitations such as a poor contrast-to-noise ratio, substantial inter-operator variability and limited acoustic window (5-7). Conversely, cardiac magnetic resonance (CMR) is considered the gold standard for comprehensive cardiac structure, function, and tissue characterization assessments. It offers an accurate quantitative evaluation of the RV function (8). Notably, the CMR feature-tracking, a novel post-processing method, can evaluate not only global LV and RV functions but also regional functions such as the interventricular septum (IVS) (9-11).

Although several studies have utilized CMR to evaluate RV function in patients with STEMI, these studies have predominately focused on the prognosis of patients with RV dysfunction (12,13). Only few studies have further explored the potential predictors associated with reduced right ventricular ejection fraction (RVEF) (14), knowledge of which can enhance our understanding of RV dysfunction and guide its treatment. Moreover, an animal study has suggested an anatomical correlation between the LV and RV, with the IVS playing a significant role in the RV's systolic function. However, there is a lack of quantitative data illustrating the relationship between the RV, IVS and LV functions (15). Therefore, this study is novel in that it aims to assess the RV structure and function using CMR imaging and identify factors that may contribute to RV dysfunction in patients with STEMI. We hypothesize that LV and IVS functions, biventricular structures, and infarct characteristics are associated with reduced RVEF. We present this article in accordance with the STROBE reporting checklist (available at https://qims.amegroups.com/article/view/10.21037/qims-23-1804/rc).

Methods

Study population

The study was conducted in accordance with the Declaration of Helsinki (as revised in 2013). The study was approved by the local ethics committee of the Chinese People's Liberation Army General Hospital (No. S202256701) and individual consent for this retrospective analysis was waived.

Two experienced radiologists (each with three years of CMR experience) searched the local picture archiving and communication system. They identified consecutive patients diagnosed with STEMI who underwent CMR imaging following a successful primary percutaneous coronary intervention (PCI) treatment between January 2012 and December 2020. STEMI diagnosis adhered to the criteria set forth by the European Society of Cardiology/American College of Cardiology (ESC/ACC) committee (16). Additional inclusion criteria were a diagnosis of STEMI for the first time, successful treatment via PCI and receipt of CMR during hospitalization (≤7 days after successful PCI). Exclusion criteria were as follows: a history of myocardial infarction and revascularization procedures (coronary artery bypass graft or PCI), unsuccessful PCI, severe arrhythmia, and insufficient CMR scan quality, obvious artifacts or incomplete magnetic resonance imaging (MRI) coverage. Ultimately, 189 patients were included in this study (*Figure 1*).

CMR protocol

CMR studies were carried out using a 1.5-Tesla scanner (Multiva, Philips, Netherlands) employing electrocardiographic gating and breath-holding during expiration and utilizing an 8-element cardiac phased-array surface coil. The standard protocols included balanced turbo

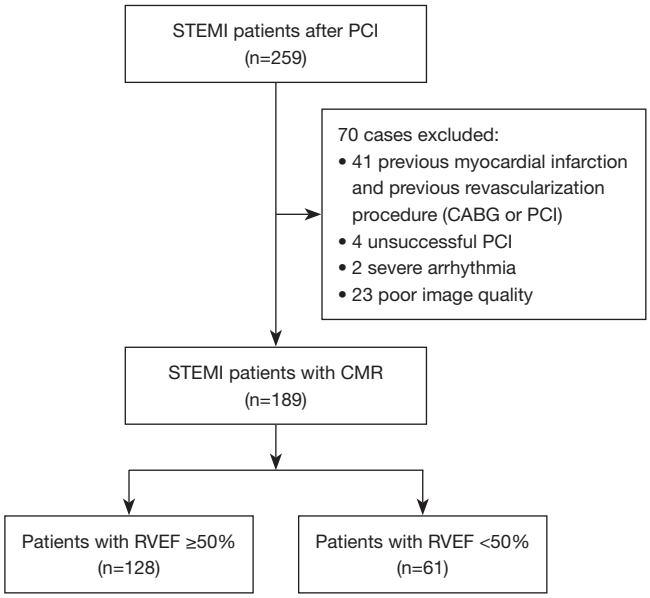

Figure 1 Study flowchart. STEMI, ST-segment elevation myocardial infarction; PCI, percutaneous coronary intervention; CABG, coronary artery bypass graft; CMR, cardiac magnetic resonance; RVEF, right ventricular ejection fraction.

field echo cine imaging and late gadolinium enhancement (LGE) imaging (Gadopentetate Dimeglumine, BeiLu, Beijing, China). LGE imaging was only used if the estimated glomerular filtration rate was ≥30 mL/min/1.73 m^2.

The imaging sequences were procured on consecutive short slices covering the LV and RV and LV 2-, 3-, 4-chamber orientations following a standardized protocol (17). The data acquisition parameters for cine imaging were as follows: cardiac phases, 25; slice thickness, 8 mm; repetition time, 3.7 ms; echo time, 1.87 ms; flip angle, 60°; the typical in-plane resolution was 1.40×1.44 mm^2. The acquisition parameters for LGE imaging included: slice thickness, 8 mm; repetition time, 6.2 ms; echo time, 3 ms; flip angle, 25°; and a typical in-plane resolution of 1.60×1.65 mm^2.

Image analysis

Cardiac MR images were analyzed using custom software (cvi42 Version 5.12.1; Circle Cardiovascular Imaging, Calgary, Alberta, Canada). Cardiac structure and function were evaluated using CMR cine imaging. The myocardial strain was computed using an automated feature-tracking post-processing method from continuous short axis and three long axis views (2-, 3-, 4-chamber orientations) of the cine image dataset. The cardiac phases of end-diastole and end-systole were automatically detected by identifying the largest and smallest cavity sizes in the LV and RV, respectively. The endocardial and epicardial contours of the LV and the endocardial contours of the RV were automatically traced with manual correction at end-diastole and -systole in short slices cine imaging by an experienced investigator blinded to clinical data. The epicardial contours of the RV were manually traced at the end-diastole and -systole by the same investigator (*Figure 2*). From these, the global and regional peak radial strains (RS), circumferential strain (CS); longitudinal strain (LS) of the LV and RV were calculated, representing the absolute maximum value of myocardial deformation in the radial, circumferential and longitudinal directions over the entire cardiac cycle. The segmental wall thickening rate (WTR) was computed by comparing the end-diastole and end-systole wall thicknesses in short-axis cine imaging according to the 17-segment model of the American Heart Association (15), excluding segment 17 (apex) (8). The global LV WTR was obtained by averaging the WTR values of all myocardial segments (8). The mass of the biventricular myocardium was calculated using outlined endocardial and epicardial contours. The biventricular end-diastolic volume (EDV), end-systolic volume (ESV), and EF were calculated using Simpson's rule according to the endocardium of the cardiac phases of end-diastole and end-systole (18). Papillary muscles were included in the ventricular cavity volume. Biventricular EDV, ESV, and myocardial mass were indexed to body surface area (18).

The location of LV infarction, RV infarction (presence or absence), and microvascular obstruction (MVO) of the LV infarction were determined using LGE imaging. Two radiologists (each with three years of CMR experience), blinded to the clinical data, independently identified the segments of LV infarction, RV infarction (*Figure 3*), and MVO of LV infarction. Any discrepancies in their readings were noted. In case of disagreement, a final decision was made by a third experienced observer. The infarct myocardium of the LV was visually evaluated and quantified using a semi-automated algorithm based on signal intensity 5 standard deviations above the mean signal intensity of the normal myocardium, as previously reported (19,20). The MVO of the LV was defined as the hypo-enhanced region within the infarct myocardium. The contours of the MVO were manually traced within the infarct myocardium; thus,

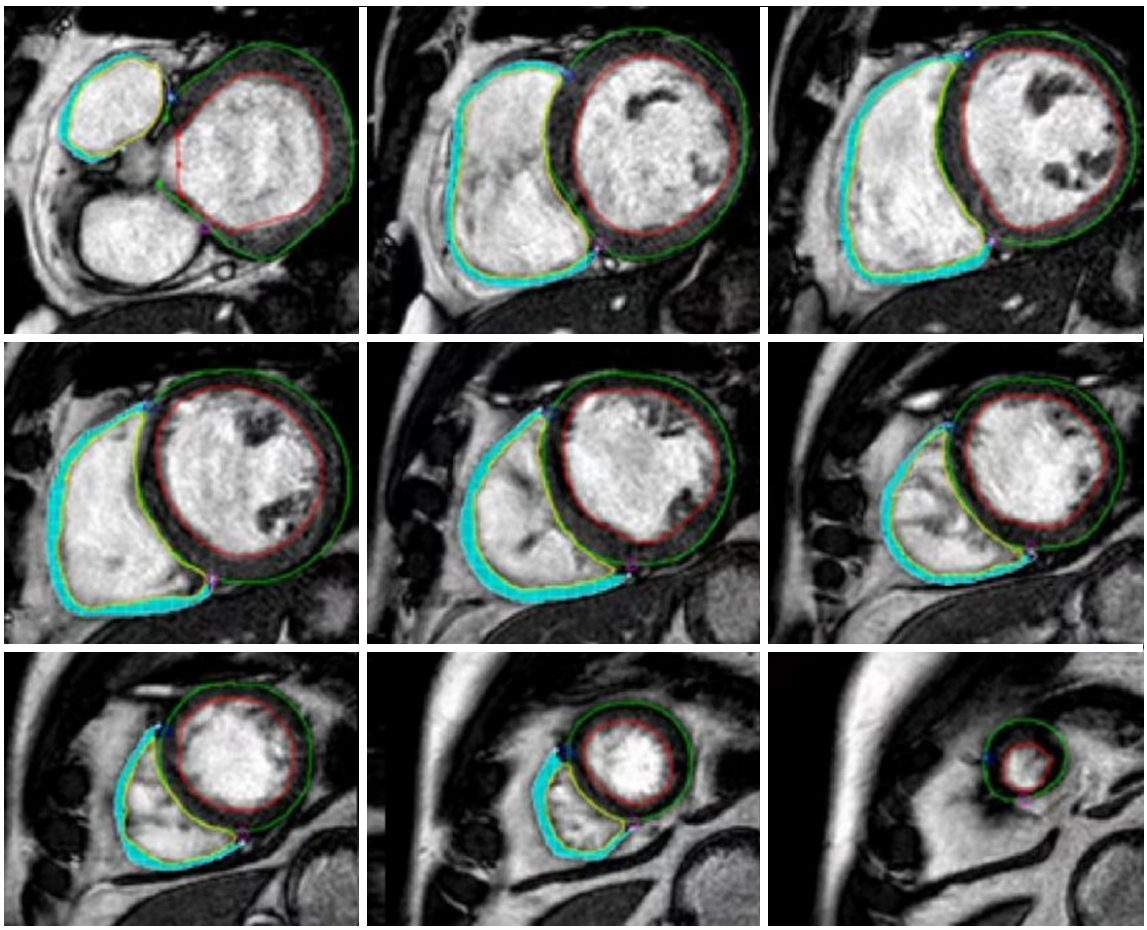

Figure 2 An illustrative example of endocardial and epicardial contours of the RV and LV at end-diastole were shown in short-axis cine imaging. The endocardial (red circles) and epicardial (green circles) contours of the LV and the endocardial (yellow circles) contours of the RV were automatically traced with manual correction. The epicardial contours of the RV were manually traced at end-diastole to ensure accurate delineation. The blue highlighted areas were the RV myocardium. RV, right ventricle; LV, left ventricle.

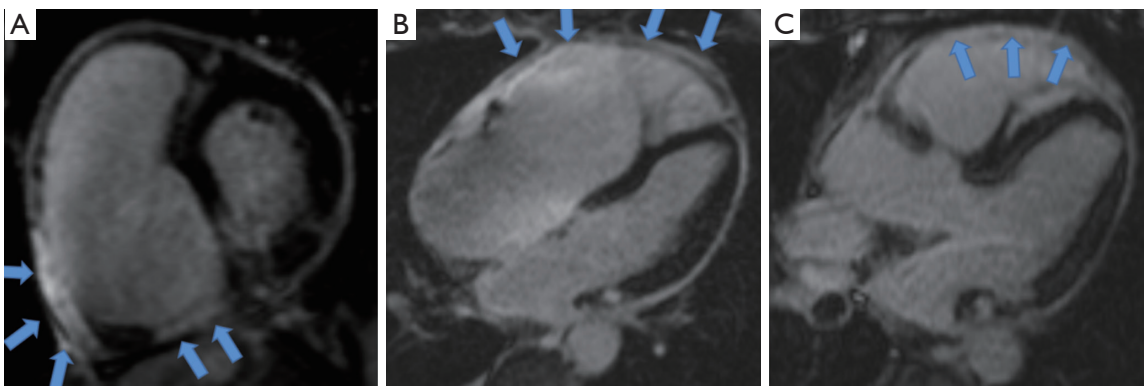

Figure 3 Typical example of RV inferior and free wall infarction on a patient with RCA occlusion by CMR LGE imaging. (A) RV inferior and free wall infarction (blue arrows) on short-axis view; (B) RV free wall infarction (blue arrows) on four-chamber view; (C) RV free wall infarction (blue arrows) on three-chamber view. RV, right ventricle; RCA, right coronary artery; CMR, cardiac magnetic resonance; LGE, late gadolinium enhancement.

the size of the MVO was included in the infarct size (21,22) (*Figure 4*).

For the systolic function and infarct size of the IVS, we used the 17-segment model of the American Heart Association (8) to analyze. In the 17-segment model, the RS, CS, LS, WTR of IVS were equivalent to the average values of LV myocardial segments 2, 3, 8, 9, and 14 (*Figure 5*). Infarct size of IVS was the sum of segments above.

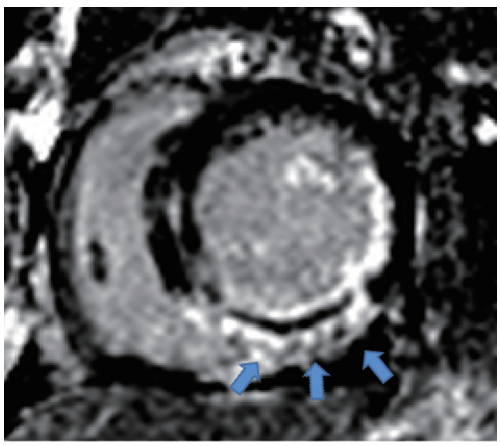

Figure 4 A prototypical instance of MVO (blue arrows) within the infarct LV inferoseptal and inferior wall due to RCA occlusion was depicted through cardiac magnetic resonance LGE imaging. MVO was clearly visible as a hypointense core within the hyperintense infarct region. MVO, microvascular obstruction; LV, left ventricle; RCA, right coronary artery; LGE, late gadolinium enhancement.

To assess the intra- and inter-observer variabilities for LV EF, LV RS, LV WTR, RVEF and RV RS, we used the intraclass correlation coefficient (ICC) in 20 randomly selected patients with acute STEMI. Intra-observer variability was assessed on cine images three months later, and inter-observer variability was assessed on the cine images by two independent radiologists.

Statistical analysis

Continuous variables were expressed as either the mean ± standard deviation or the median with the interquartile range, while categorical variables were presented as frequencies and percentages. The differences in continuous variables between STEMI patients with RVEF <50% and those with RVEF ≥50% were compared using the independent-sample *t*-test or Wilcoxon rank-sum test. In contrast, the chi-square test or Fisher's exact test was employed to compare categorical variables. Univariate and multivariate linear regression analyses were performed to identify independent predictors of RVEF. According to the research, we defined RVEF <50% as RV dysfunction (23). The area under the curve (AUC) was evaluated using receiver operating characteristic (ROC) curve analysis to predict RV dysfunction. All statistical analyses were conducted using the SPSS statistical package (SPSS Statistics 23.0; IBM, Armonk, New York, USA). All tests were two-sided, and P values less than 0.05 was considered statistically significant.

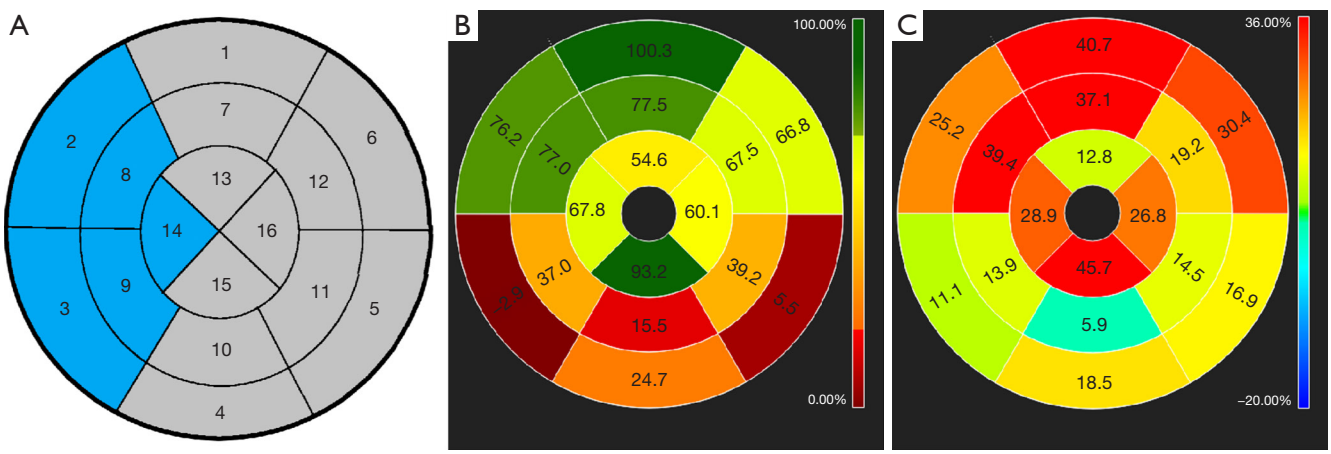

Figure 5 Schematic diagram illustrating the measurement of left ventricular segmental wall thickening rate and strains. (A) Schematic diagram of the IVS, the IVS were the segments 2, 3, 8, 9 and 14 on the 17-segment model. (B) Representative bull's eye maps for wall thickening rate. (C) Representative bull's eye maps for radial peak strain. IVS, interventricular septum.

Results

Study population

A total of 259 consecutive patients with STEMI were screened between January 2012 and December 2020. Of these, 70 patients were excluded for various reasons, as shown in *Figure 1*. Finally, 189 patients with STEMI were included in the analysis.

Baseline characteristics

The baseline characteristics of the study population are presented in *Table 1*. Most of the study population was male (87.83%), with a mean age of 55.92±10.92 years. Using a cut-off value of RVEF =50%, the study population was divided into RVEF <50% or RVEF ≥50% groups, and 32.28% (61/189) of patients had RVEF <50%. Compared with those RVEF ≥50%, patients with RVEF <50% were also more likely to have a culprit lesion in the right coronary artery (RCA) (59.02% *vs.* 37.50%; P=0.01) and to have a drinking habit (40.98% *vs.* 25.78%; P=0.03). The group with RVEF <50% also had a higher proportion of male patients (95.08% *vs.* 84.38%; P=0.04). Furthermore, patients with RVEF <50% had higher maximum creatine kinase-MB (CK-MB) levels (274.37±213.33 *vs.* 207.33±154.89; P=0.02) and peak troponin levels (10.43±10.83 *vs.* 6.53±6.20; P=0.01) compared to patients with RVEF ≥50%. Notably, more patients with RVEF <50% used diuretics during treatment (60.66% *vs.* 42.19%; P=0.02).

Comparison of LV, IVS, and RV CMR characteristics between the groups with RVEF <50% and RVEF ≥50%

In patients with RVEF <50%, there was a significantly higher LV end-systolic volume index (ESVI) (49.74±18.78 *vs.* 40.50±11.51 mL/m^2; P<0.001) and LV myocardial mass index (MMI) (62.94±11.73 *vs.* 58.88±11.49 g/m^2; P=0.03) compared with those RVEF ≥50% (*Table 2*). Moreover, patients with RVEF <50% exhibited a significantly lower LVEF (41.42%±10.11% *vs.* 49.22%±8.17%; P<0.001), LV RS (19.95%±6.20% *vs.* 23.91%±6.33%; P<0.001), LV CS (–12.78%±3.27% *vs.* –14.76%±2.82%; P<0.001) and LV WTR (38.63%±14.59% *vs.* 46.90%±13.06%; P<0.001). Although the LV MVO size did not differ significantly between the groups (1.59±3.84 *vs.* 0.92±1.93 mL; P=0.11), the LV infarct size was greater in the group with RVEF <50% (30.51±17.92 *vs.* 22.35±15.15 mL; P=0.001). Regarding the IVS, the group with RVEF <50% demonstrated a significantly lower WTR (25.80%±13.37% *vs.* 32.19%±14.46%; P<0.001) than the group with RVEF ≥50%.

Patients with RVEF <50% also displayed a significantly higher RV ESVI (27.88±9.56 *vs.* 26.47±6.95 mL/m^2; P<0.001), lower RV RS (20.28%±6.43% *vs.* 29.71%±8.09%; P<0.001), RV CS (–12.18%±3.47% *vs.* –15.69%±4.77%; P<0.001) and RV LS (–16.94%±6.77% *vs.* –19.61%±9.13%; P=0.04) compared with those with RVEF ≥50%. Among the 189 STEMI patients, RV infarction was detected in 42 patients (22.22%, 42/189), with 26 of these patients (61.90%, 26/42) having an infarct-related artery RCA and 16 patients (38.10%, 16/42) with a non-RCA. Besides, of the 42 STEMI patients with RV infarction, the incidence of RV infarction was higher in the group with RVEF <50% (32.79%, 20/61) compared to the group with RVEF ≥50% (17.19%, 22/128) (P=0.02).

Predictors of RVEF

Table 3 presents the results from univariate and multivariate linear regression analyses, identifying the predictors of RVEF. Male gender, the culprit lesion in the RCA, maximum CK-MB, peak troponin, LV ESVI, LV EF, LV WTR, LV RS, LV CS, LV LS, LV infarct size, the presence of LV MVO, IVS WTR, IVS RS, IVS LS and the presence of RV infarction were found to be independently associated with RVEF in the univariate linear analysis. The univariate analysis informed the selection of covariates for the subsequent multivariate analysis, including those with P<0.05. Multivariable linear regression analysis identified LV EF, IVS WTR and IVS RS as significant predictors for RVEF, while male gender, the culprit lesion in the RCA, peak troponin were negative predictors for RVEF.

Based on the previous research, we defined RVEF <50% as RV dysfunction (23), and then used the ROC curve to evaluate the predictive ability of clinical and CMR parameters for RV dysfunction. Notably, peak troponin [AUC 0.62; 95% confidence interval (CI): 0.54–0.71], LV EF (AUC 0.72; 95% CI: 0.64–0.80), LV RS (AUC 0.66; 95% CI: 0.58–0.75), LV CS (AUC 0.67; 95% CI: 0.58–0.76), LV WTR (AUC 0.68; 95% CI: 0.60–0.76), and IVS WTR (AUC 0.63; 95% CI: 0.54–0.72) demonstrated higher AUC values for predicting RV dysfunction (*Figure 6*).

Reproducibility assessment

The reproducibility of LV EF, LV RS, LV WTR, RVEF

Table 1 Demographic characteristics according to RVEF

Characteristic	All patients (n=189)	RVEF ≥50% (n=128)	RVEF <50% (n=61)	P
Clinical parameters				
Age (years)	55.92±10.92	55.90±10.89	55.95±11.08	0.98
Male	166 (87.83)	108 (84.38)	58 (95.08)	0.04*
Body mass index (kg/m^2)	25.88±3.43	25.93±3.21	35.79±3.87	0.80
Family history of CAD	24 (12.70)	17 (13.28)	7 (11.48)	0.73
Hypertension	98 (51.85)	63 (49.22)	35 (57.38)	0.30
Hypercholesterolemia	43 (22.75)	33 (25.78)	10 (16.39)	0.15
Diabetes mellitus	30 (15.87)	21 (16.41)	9 (14.75)	0.77
Smoking	117 (61.90)	78 (60.94)	39 (63.93)	0.69
Drinking	58 (30.69)	33 (25.78)	25 (40.98)	0.03*
Heart rate, beats/min	71.36±11.59	70.79±11.23	72.57±12.33	0.32
Systolic blood pressure (mmHg)	131.13±19.16	128±130.68	61±132.07	0.63
Killip class >I	18 (9.52)	12 (9.38)	6 (9.84)	0.92
Intervention				
Door-to-balloon time (min)	119.08±125.93	108.71±84.31	140.86±184.20	0.20
Multivessel disease	126 (66.67)	87 (67.97)	39 (63.93)	0.58
Culprit lesion in the RCA	84 (44.44)	48 (37.50)	36 (59.02)	0.01*
TIMI flow pre-PCI ≤2	177 (93.65)	119 (92.97)	58 (95.08)	0.75
TIMI flow post-PCI ≤2	3 (1.59)	2 (1.56)	1 (1.64)	1.00
Stents, total number, n	1.65±0.91	1.64±0.90	1.67±0.93	0.83
Blood results				
NT-pro BNP, pg/mL (IQR)	1,678.13±1,526.31	1,653.87±1,452.15	1,729.03±1,682.86	0.75
Maximum CK-MB (U/L)	228.96±178.10	207.33±154.89	274.37±213.33	0.02*
Peak troponin (mg/L)	7.79±8.17	6.53±6.20	10.43±10.83	0.01*
Medication use				
Aspirin	188 (99.49)	127 (99.22)	61 (100)	0.68
Clopidogrel/ticagrelor	188 (99.49)	127 (99.22)	61 (100)	0.68
Statin	188 (99.49)	127 (99.22)	61 (100)	0.68
ACEI/ARB	78 (41.27)	47 (36.72)	31 (50.82)	0.07
Beta-blockers	164 (86.77)	112 (87.50)	52 (85.25)	0.67
Diuretic	91 (48.15)	54 (42.19)	37 (60.66)	0.02*

Results are reported as mean ± SD or number (frequency). *, P<0.05. RVEF, right ventricle ejection fraction; CAD, coronary artery disease; RCA, right coronary artery; TIMI, thrombolysis in myocardial infarction; PCI, percutaneous coronary intervention; NT-pro BNP, N-terminal pro b-type natriuretic peptide; IQR, interquartile range; CK-MB, creatine kinase-MB; ACEI, angiotensin-converting enzyme inhibitors; ARB, angiotensin receptor blocker; SD, standard deviation.

Table 2 CMR features of the study population

Characteristic	All patients (n=189)	RVEF ≥50% (n=128)	RVEF <50% (n=61)	P
LV EF (%)	46.70±9.55	49.22±8.17	41.42±10.11	<0.001*
LV EDVI (mL/m^2)	80.86±19.29	79.40±17.66	83.93±22.18	0.13
LV ESVI (mL/m^2)	43.48±14.86	40.50±11.51	49.74±18.78	<0.001*
LV myocardial mass index (g/m^2)	60.19±11.69	58.88±11.49	62.94±11.73	0.03*
LV RS (%)	22.63±6.54	23.91±6.33	19.95±6.20	<0.001*
LV CS (%)	−14.12±3.11	−14.76±2.82	−12.78±3.27	<0.001*
LV LS (%)	−11.75±3.75	−12.06± 3.70	−11.10±3.78	0.10
LV WTR (%)	44.23±14.07	46.90±13.06	38.63±14.59	<0.001*
LV infarct size (mL)	24.99±16.50	22.35±15.15	30.51±17.92	0.001*
LV MVO	67 (35.45)	40 (31.25)	27 (44.26)	0.08
LV MVO size (mL)	1.13±2.71	0.92±1.93	1.59±3.84	0.11
IVS RS (%)	22.5±10.0	23.39±10.09	20.59±9.64	0.07
IVS WTR (%)	30.12±14.40	32.19±14.46	25.80±13.37	<0.001*
IVS infarct size (mL)	19.45±18.80	18.76±18.09	20.89±20.29	0.47
RV EF (%)	53.29±11.15	59.28 ±6.76	40.71±7.43	<0.001*
RV EDVI (mL/m^2)	66.56±19.18	65.68±18.86	68.40±19.87	0.37
RV ESVI (mL/m^2)	31.00±11.43	26.47±6.95	27.88±9.56	<0.001*
RV myocardial mass index (g/m^2)	12.36±4.07	12.23±3.89	12.62±4.46	0.54
RV RS (%)	26.66±8.77	29.71±8.09	20.28±6.43	<0.001*
RV CS (%)	−14.55±4.68	−15.69±4.77	−12.18±3.47	<0.001*
RV LS (%)	−18.75±8.51	−19.61±9.13	−16.94±6.77	0.04*
RV infarction	42 (22.22)	22 (17.19)	20 (32.79)	0.02*

Results are reported as mean ± SD or number (frequency). *, P<0.05. CMR, cardiac magnetic resonance; RVEF, right ventricle ejection fraction; LV, left ventricle; EF, ejection fraction; EDVI, end-diastolic volume index; ESVI, end-systolic volume index; RS, radial peak strain; CS, circumferential peak strain; LS, longitudinal peak strain; WTR, wall thickening rate; MVO, microvascular obstruction; IVS, interventricular septum; SD, standard deviation.

and RV RS was assessed for both intra- and inter-observer agreement. The results showed high agreement for intra- and inter-observer reproducibility for all parameters (*Table 4*).

Discussion

In this study, we evaluated the structure, function, and tissue characteristics of the RV, LV, and IVS using CMR and investigated the factors affecting RVEF in patients with acute STEMI. Our key findings can be summarized as follows: first, 32.3% of patients with acute STEMI exhibited reduced RVEF, alongside impaired LV and IVS functions. Second, systolic function of the LV and IVS, peak troponin, and culprit lesions in the RCA were strongly associated with RV systolic function.

Assessment of cardiac function and myocardial tissue characteristics by CMR

Assessing the structure and systolic function of the right ventricle (RV) has been challenging due to its complex geometry and thin wall thickness of only 3–4 mm (24). Despite these hurdles, advancements in CMR technology, such as feature tracking technology, have enabled

Table 3 Univariate and multivariate linear regression analysis for the RVEF

Characteristic	Univariate		Multivariate	
	P	β (CI)	P	β (CI)
Age (years)	0.99	−0.001 (−0.15 to 0.15)		
Male	0.01	6.55 (1.74 to 11.37)	0.001	−6.20 (−9.87 to −2.53)
Body mass index (kg/m^2)	0.17	−0.32 (−0.79 to 0.14)		
Family history of CAD	0.36	2.25 (−2.56 to 7.06)		
Hypertension	0.46	−1.18 (−4.32 to 1.97)		
Hypercholesterolemia	0.26	2.18 (−1.63 to 5.99)		
Diabetes mellitus	0.9	−0.27 (−4.66 to 4.12)		
Smoking	0.37	−1.50 (−4.80 to 1.80)		
Drinking	0.15	−2.41 (−5.68 to 0.86)		
Door-to-balloon time (min)	0.23	0.15 (−0.10 to 0.39)		
Culprit lesion in the RCA	0.001	−5.20 (−8.34 to −2.06)	<0.001	−8.33 (−10.88 to −5.81)
NT-proBNP (pg/mL)	0.28	−0.001 (−0.002 to 0.00)		
Maximum CK-MB (U/L)	0.004	−0.01 (−0.02 to −0.004)		
Peak troponin (mg/L)	0.000	−0.40 (−0.57 to −0.20)	0.033	−0.18 (−0.34 to −0.02)
LV EDVI (mL/m^2)	0.866	0.01 (−0.08 to 0.09)		
LV ESVI (mL/m^2)	0.000	−0.21 (−0.3 to −0.11)		
LV myocardial mass index (g/m^2)	0.284	−0.08 (−0.21 to 0.06)		
LV EF (%)	<0.001	0.56 (0.42 to 0.71)	<0.001	0.71 (0.53 to 0.89)
LV WTR (%)	<0.001	0.28 (0.18 to 0.39)		
LV RS (%)	<0.001	0.69 (0.46 to 0.91)		
LV CS (%)	<0.001	−1.44 (−1.91 to −0.97)		
LV LS (%)	<0.001	−0.65 (−1.07 to −0.23)		
LV infarct size (mL)	0.01	−0.14 (−0.23 to −0.04)		
LV MVO	0.002	−5.12 (−8.39 to −1.85)		
LV MVO size (mL)	0.09	−0.52 (−1.11 to 0.74)		
IVS WTR (%)	<0.001	0.24 (0.14 to 0.35)	0.03	0.13 (0.02 to 0.25)
IVS RS (%)	0.01	0.21 (0.05 to 0.37)	0.002	0.30 (0.48 to 0.11)
IVS CS (%)	0.75	−0.01 (−0.04 to 0.03)		
IVS LS (%)	0.03	−0.32 (−0.61 to −0.03)		
IVS infarct size (mL)	0.06	−0.47 (−0.96 to 0.03)		
RV Infarction	0.01	−5.44 (−9.23 to −1.66)		

RVEF, right ventricle ejection fraction; CI, confidence interval; CAD, coronary artery disease; RCA, right coronary artery; NT-pro BNP, N-terminal pro b-type natriuretic peptide; CK-MB, creatine kinase-MB; LV, left ventricle; EDVI, end-diastolic volume index; ESVI, end-systolic volume index; EF, ejection fraction; WTR, wall thickening rate; RS, radial peak strain; CS, circumferential peak strain; LS, longitudinal peak strain; MVO, microvascular obstruction; IVS, interventricular septum; RV, right ventricle.

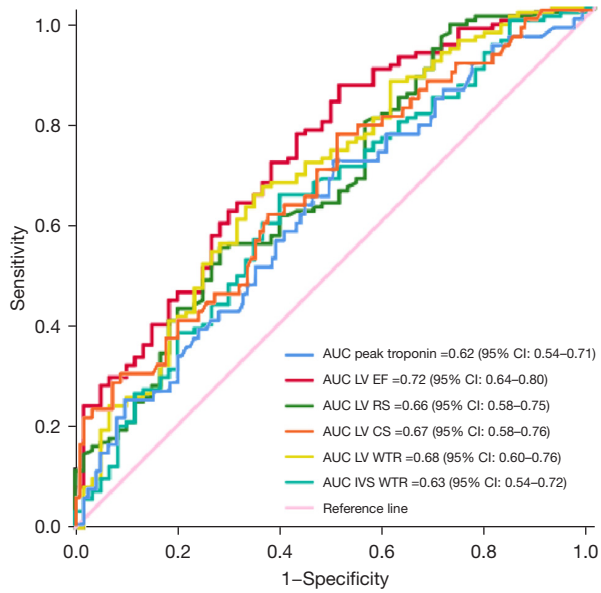

Figure 6 Discriminative RV dysfunction power of peak troponin, LV EF, LV RS, LV CS, LV WTR, and IVS WTR. AUC, area under the curve; LV, left ventricle; EF, ejection fraction; RS, radial peak strain; CS, circumferential peak strain; WTR, wall thickening rate; IVS, interventricular septum; RV, right ventricle.

Table 4 Reproducibility analysis of some cardiac magnetic resonance parameters

Characteristic	ICC (intra-observer reproducibility)	ICC (inter-observer reproducibility)
LV EF (%)	0.97	0.86
LV RS (%)	0.98	0.82
LV WTR (%)	0.96	0.85
RV EF (%)	0.92	0.85
RV RS (%)	0.91	0.82

ICC, intra-class correlation coefficient; LV, left ventricle; EF, ejection fraction; RS, radial peak strain; WTR, wall thickening rate; RV, right ventricle.

objective and quantitative evaluation of RV myocardial deformation (25). Furthermore, CMR-FT can assess global and regional myocardial function (8,26,27). In this study, we evaluated the regional RS and WTR of the IVS. We found that the IVS WTR was more impaired in STEMI patients exhibiting RVEF <50% than those with RVEF ≥50%. This suggests a potential relationship between the function of the IVS and RV function. Additionally, CMR can detect LGE in the RV, a feature not achievable using echocardiography (19,20). In this study, we discovered RV infarction in 42 (22.22%, 42/189) STEMI patients, with the RCA identified as the culprit vessel in 26 cases (61.90%) and non-RCA in 16 cases (38.10%). Our findings also supported ideas from previous study that RV infarction can occur in patients with an RCA culprit vessel and those with non-RCA culprit vessels (28). For the diagnosis and evaluation of the extent of myocardial infarction, previous studies have found that necrosis-avid agent has provided unique advantages in single photon emission computed tomography. Although this is preclinical evidence, it still has high clinical value and research prospects (29,30).

The factors affecting the RVEF

Compared with STEMI patients without RV dysfunction, those exhibiting RV dysfunction have shown a more than 4-fold increase in long-term mortality (12). Therefore, identifying factors influencing RV function in patients with STEMI is crucial. Our study found that peak troponin was a crucial determinant of RV dysfunction, which was attributed to patients with elevated troponin having larger myocardial infarct sizes, so relatively more severe impairment of myocardial contraction. Roifman et al.'s previous study (14) reported diabetes as an independent predictor of reduced RVEF post-STEMI. However, our study did not find a correlation, possibly due to a lower incidence of diabetes in our cohort (15.87%) compared with that of Roifman's study (30.0%). Besides the peak troponin, we found a strong correlation between the culprit lesion in the RCA and RVEF, a finding that could be attributed to the RV's perfusion characteristics. As the RCA supplies 70.0–80.0% of the RV's perfusion, its occlusion, leading to RV ischemia, is associated with reduced RVEF (31). Although patients with reduced RVEF had a high incidence of RV infarction, there was no significant relationship between RV infarction and reduced RVEF in multivariate regression analysis. In our study, the size of RV infarction was usually small, therefore its impact on myocardial contractility was slight.

Previous anatomical studies have shown an interactive relationship between RV and LV shape and function, suggesting that alterations in one ventricle can influence the other (29,30). Recently, experimental models have demonstrated that LV contraction can contribute 20.0% to 40.0% of RV stroke volume (13,32,33). Remarkably, in addition to LVEF, IVS WTR was also associated with RVEF in our study, this correlation remained even after adjusting for other crucial determinants such as the culprit

lesions in the RCA. Additionally, Popescu *et al.* (34) found that an improvement in IVS performance correlated with the recovery of RV function.

The implications of the study's findings

The study has found that there are some factors that can affect RVEF in STEMI patients. These include systolic function of the LV and IVS, peak troponin, and culprit lesions in the RCA. Moving forward, more research could be conducted to check the accuracy of these predictors and improve the risk stratification models for identifying people who may be at a higher risk of suffering from RV dysfunction after experiencing an acute ST-segment elevation myocardial infarction. Such improved prediction models could also help with clinical decision making and choosing ideal treatment strategies.

Limitations

Despite these significant findings, there are two limitations in this study. First, we conducted only a qualitative analysis of RV infarction, because it was difficult to quantitatively explore RV infarct size. Therefore, the relationship between reduced RVEF and RV infarction may have been underestimated. Second, this study was retrospective and conducted at a single site; therefore, prospective studies conducted across multiple centers are needed to validate the current findings.

Conclusions

In conclusion, RV dysfunction was detected in 32.28% of STEMI patients. Patients with acute STEMI and reduced RVEF had impaired LV and IVS functions. Systolic function of the LV and IVS, peak troponin, and culprit lesions in the RCA were independent predictors of post-MI RV dysfunction. These findings support the systemic evaluation of RV function using CMR in patients with acute STEMI.

Acknowledgments

We thank Xiuzheng Yue of Department of Clinical Science, Philips Healthcare for his skilled assistance during the CMR images acquisition.

Funding: This research was supported by the New Technology and Business of Chinese People's Liberation Army General Hospital (No. 20230116).

Footnote

Reporting Checklist: The authors have completed the STROBE reporting checklist. Available at https://qims.amegroups.com/article/view/10.21037/qims-23-1804/rc

Conflicts of Interest: All authors have completed the ICMJE uniform disclosure form (available at https://qims.amegroups.com/article/view/10.21037/qims-23-1804/coif). All authors report that the study was supported by New Technology and Business of Chinese People's Liberation Army General Hospital (No. 20230116). The authors have no other conflicts of interest to declare.

Ethical Statement: The authors are accountable for all aspects of the work in ensuring that questions related to the accuracy or integrity of any part of the work are appropriately investigated and resolved. The study was conducted in accordance with the Declaration of Helsinki (as revised in 2013). The study was approved by the local ethics committee of the Chinese People's Liberation Army General Hospital (No. S202256701) and individual consent for this retrospective analysis was waived.

References

1. Ibanez B, James S, Agewall S, Antunes MJ, Bucciarelli-Ducci C, Bueno H, Caforio ALP, Crea F, Goudevenos JA, Halvorsen S, Hindricks G, Kastrati A, Lenzen MJ, Prescott E, Roffi M, Valgimigli M, Varenhorst C, Vranckx P, Widimský P; ESC Scientific Document Group. 2017 ESC Guidelines for the management of acute myocardial infarction in patients presenting with ST-segment elevation: The Task Force for the management of acute myocardial infarction in patients presenting with ST-segment elevation of the European Society of Cardiology (ESC). Eur Heart J 2018;39:119-77.
2. Reindl M, Tiller C, Holzknecht M, Lechner I, Eisner D, Riepl L, Pamminger M, Henninger B, Mayr A, Schwaiger

JP, Klug G, Bauer A, Metzler B, Reinstadler SJ. Global longitudinal strain by feature tracking for optimized prediction of adverse remodeling after ST-elevation myocardial infarction. Clin Res Cardiol 2021;110:61-71.
3. Ondrus T, Kanovsky J, Novotny T, Andrsova I, Spinar J, Kala P. Right ventricular myocardial infarction: From pathophysiology to prognosis. Exp Clin Cardiol 2013;18:27-30.
4. Namana V, Gupta SS, Abbasi AA, Raheja H, Shani J, Hollander G. Right ventricular infarction. Cardiovasc Revasc Med 2018;19:43-50.
5. Javed S, Rajani AR, Govindaswamy P, Radaideh GA, Abubaraka HA, Qureshi TI, Arshad HB. Right ventricular involvement in patients with inferior myocardial infarction, correlation of electrocardiographic findings with echocardiography data. J Pak Med Assoc 2017;67:442-5.
6. Goedemans L, Hoogslag GE, Abou R, Schalij MJ, Marsan NA, Bax JJ, Delgado V. ST-Segment Elevation Myocardial Infarction in Patients With Chronic Obstructive Pulmonary Disease: Prognostic Implications of Right Ventricular Systolic Dysfunction as Assessed with Two-Dimensional Speckle-Tracking Echocardiography. J Am Soc Echocardiogr 2019;32:1277-85.
7. Abdeltawab AA, Elmahmoudy AM, Elnammas W, Mazen A. Assessment of right ventricular function after successful revascularization for acute anterior myocardial infarction without right ventricular infarction by echocardiography. J Saudi Heart Assoc 2019;31:261-8.
8. Podlesnikar T, Pizarro G, Fernández-Jiménez R, Montero-Cabezas JM, Greif N, Sánchez-González J, Bucciarelli-Ducci C, Marsan NA, Fras Z, Bax JJ, Fuster V, Ibáñez B, Delgado V. Left ventricular functional recovery of infarcted and remote myocardium after ST-segment elevation myocardial infarction (METOCARD-CNIC randomized clinical trial substudy). J Cardiovasc Magn Reson 2020;22:44.
9. Li H, Zheng Y, Peng X, Liu H, Li Y, Tian Z, Hou Y, Jin S, Huo H, Liu T. Heart failure with preserved ejection fraction in post myocardial infarction patients: a myocardial magnetic resonance (MR) tissue tracking study. Quant Imaging Med Surg 2023;13:1723-39.
10. Chen X, Pan J, Shu J, Zhang X, Ye L, Chen L, Hu Y, Yu R. Prognostic value of regional strain by cardiovascular magnetic resonance feature tracking in hypertrophic cardiomyopathy. Quant Imaging Med Surg 2022;12:627-41.
11. Wen X, Gao Y, Guo Y, Zhang Y, Zhang Y, Shi K, Li Y, Yang Z. Assessing right ventricular peak strain in myocardial infarction patients with mitral regurgitation by cardiac magnetic resonance feature tracking. Quant Imaging Med Surg 2024;14:3018-32.
12. Larose E, Ganz P, Reynolds HG, Dorbala S, Di Carli MF, Brown KA, Kwong RY. Right ventricular dysfunction assessed by cardiovascular magnetic resonance imaging predicts poor prognosis late after myocardial infarction. J Am Coll Cardiol 2007;49:855-62.
13. Sanz J, Sánchez-Quintana D, Bossone E, Bogaard HJ, Naeije R. Anatomy, Function, and Dysfunction of the Right Ventricle: JACC State-of-the-Art Review. J Am Coll Cardiol 2019;73:1463-82.
14. Roifman I, Ghugre N, Zia MI, Farkouh ME, Zavodni A, Wright GA, Connelly KA. Diabetes is an independent predictor of right ventricular dysfunction post ST-elevation myocardial infarction. Cardiovasc Diabetol 2016;15:34.
15. Apitz C, Honjo O, Humpl T, Li J, Assad RS, Cho MY, Hong J, Friedberg MK, Redington AN. Biventricular structural and functional responses to aortic constriction in a rabbit model of chronic right ventricular pressure overload. J Thorac Cardiovasc Surg 2012;144:1494-501.
16. Thygesen K, Alpert JS, Jaffe AS, Simoons ML, Chaitman BR, White HD, et al. Third universal definition of myocardial infarction. Circulation 2012;126:2020-35.
17. Kramer CM, Barkhausen J, Flamm SD, Kim RJ, Nagel E; Society for Cardiovascular Magnetic Resonance Board of Trustees Task Force on Standardized Protocols. Standardized cardiovascular magnetic resonance imaging (CMR) protocols, society for cardiovascular magnetic resonance: board of trustees task force on standardized protocols. J Cardiovasc Magn Reson 2008;10:35.
18. Hallén J, Jensen JK, Fagerland MW, Jaffe AS, Atar D. Cardiac troponin I for the prediction of functional recovery and left ventricular remodelling following primary percutaneous coronary intervention for ST-elevation myocardial infarction. Heart 2010;96:1892-7.
19. Wang Q, Wang J, Ma Y, Wang P, Li Y, Tian J, Yue X, Su G, Li B. Predictive value of myocardial strain on myocardial infarction size by cardiac magnetic resonance imaging in ST-segment elevation myocardial infarction with preserved left ventricular ejection fraction. Front Pharmacol 2022;13:1015390.
20. Houard L, Benaets MB, de Meester de Ravenstein C, Rousseau MF, Ahn SA, Amzulescu MS, Roy C, Slimani A, Vancraeynest D, Pasquet A, Vanoverschelde JJ, Pouleur AC, Gerber BL. Additional Prognostic Value of 2D Right Ventricular Speckle-Tracking Strain for Prediction of Survival in Heart Failure and Reduced Ejection Fraction:

A Comparative Study With Cardiac Magnetic Resonance. JACC Cardiovasc Imaging 2019;12:2373-85.
21. Holzknecht M, Reindl M, Tiller C, Reinstadler SJ, Lechner I, Pamminger M, Schwaiger JP, Klug G, Bauer A, Metzler B, Mayr A. Global longitudinal strain improves risk assessment after ST-segment elevation myocardial infarction: a comparative prognostic evaluation of left ventricular functional parameters. Clin Res Cardiol 2021;110:1599-611.
22. Reindl M, Reinstadler SJ, Feistritzer HJ, Theurl M, Basic D, Eigler C, Holzknecht M, Mair J, Mayr A, Klug G, Metzler B. Relation of Low-Density Lipoprotein Cholesterol With Microvascular Injury and Clinical Outcome in Revascularized ST-Elevation Myocardial Infarction. J Am Heart Assoc 2017;6:e006957.
23. Pavlicek M, Wahl A, Rutz T, de Marchi SF, Hille R, Wustmann K, Steck H, Eigenmann C, Schwerzmann M, Seiler C. Right ventricular systolic function assessment: rank of echocardiographic methods vs. cardiac magnetic resonance imaging. Eur J Echocardiogr 2011;12:871-80.
24. McLeod K, Wall S, Leren IS, Saberniak J, Haugaa KH. Ventricular structure in ARVC: going beyond volumes as a measure of risk. J Cardiovasc Magn Reson 2016;18:73.
25. Schuster A, Hor KN, Kowallick JT, Beerbaum P, Kutty S. Cardiovascular Magnetic Resonance Myocardial Feature Tracking: Concepts and Clinical Applications. Circ Cardiovasc Imaging 2016;9:e004077.
26. Lange T, Stiermaier T, Backhaus SJ, Boom PC, Kowallick JT, de Waha-Thiele S, Lotz J, Kutty S, Bigalke B, Gutberlet M, Feistritzer HJ, Desch S, Hasenfuß G, Thiele H, Eitel I, Schuster A. Functional and prognostic implications of cardiac magnetic resonance feature tracking-derived remote myocardial strain analyses in patients following acute myocardial infarction. Clin Res Cardiol 2021;110:270-80.
27. Zhang L, Mandry D, Chen B, Huttin O, Hossu G, Wang H, Beaumont M, Girerd N, Felblinger J, Odille F. Impact of microvascular obstruction on left ventricular local remodeling after reperfused myocardial infarction. J Magn Reson Imaging 2018;47:499-510.
28. Miszalski-Jamka T, Klimeczek P, Tomala M, Krupiński M, Zawadowski G, Noelting J, Lada M, Sip K, Banyś R, Mazur W, Kereiakes DJ, Zmudka K, Pasowicz M. Extent of RV dysfunction and myocardial infarction assessed by CMR are independent outcome predictors early after STEMI treated with primary angioplasty. JACC Cardiovasc Imaging 2010;3:1237-46.
29. Yang S, Ma J, Li T, Wang P, Wang X, Zhang J, Ni Y, Shao H. Radioiodinated hypericin as a tracer for detection of acute myocardial infarction: SPECT-CT imaging in a swine model. J Nucl Cardiol 2022;29:3432-9.
30. Fonge H, Vunckx K, Wang H, Feng Y, Mortelmans L, Nuyts J, Bormans G, Verbruggen A, Ni Y. Non-invasive detection and quantification of acute myocardial infarction in rabbits using mono-[123I]iodohypericin microSPECT. Eur Heart J 2008;29:260-9.
31. Mauger C, Gilbert K, Lee AM, Sanghvi MM, Aung N, Fung K, Carapella V, Piechnik SK, Neubauer S, Petersen SE, Suinesiaputra A, Young AA. Right ventricular shape and function: cardiovascular magnetic resonance reference morphology and biventricular risk factor morphometrics in UK Biobank. J Cardiovasc Magn Reson 2019;21:41.
32. Konstam MA, Kiernan MS, Bernstein D, Bozkurt B, Jacob M, Kapur NK, Kociol RD, Lewis EF, Mehra MR, Pagani FD, Raval AN, Ward C; American Heart Association Council on Clinical Cardiology; Council on Cardiovascular Disease in the Young; and Council on Cardiovascular Surgery and Anesthesia. Evaluation and Management of Right-Sided Heart Failure: A Scientific Statement From the American Heart Association. Circulation 2018;137:e578-622.
33. Naeije R, Badagliacca R. The overloaded right heart and ventricular interdependence. Cardiovasc Res 2017;113:1474-85.
34. Popescu BA, Antonini-Canterin F, Temporelli PL, Giannuzzi P, Bosimini E, Gentile F, Maggioni AP, Tavazzi L, Piazza R, Ascione L, Stoian I, Cervesato E, Popescu AC, Nicolosi GL; GISSI-3 Echo Substudy Investigators. Right ventricular functional recovery after acute myocardial infarction: relation with left ventricular function and interventricular septum motion. GISSI-3 echo substudy. Heart 2005;91:484-8.

Cite this article as: Zhao Y, Cui J, Zhang X, Li J, Yang J, Li T. Right ventricular function and determining factors of dysfunction in ST-segment-elevation myocardial infarction: a cross-sectional study with cardiac magnetic resonance imaging (MRI). Quant Imaging Med Surg 2024;14(9):6895-6907. doi: 10.21037/qims-23-1804

